Near Unity Quantum Yield of Light-driven Redox Mediator Reduction and Efficient H$_2$ Generation Using Colloidal Nanorod Heterostructures

Haiming Zhu, Nianhui Song, Hongjin Lv, Craig L. Hill and Tianquan Lian*

Supporting Information List:

S1. Materials and methods

Nanocrystal (NC) synthesis

CdSe seed: High quality wurtzite CdSe seeds were synthesized following a literature procedure.[1] Briefly, 0.06 g Cadmium Oxide (CdO), 0.28 g Octadecylphosphonic acid (ODPA) and 3g Trioctylphosphine oxide (TOPO) were mixed in a 25 mL flask and heated to 300 °C under Argon flow. After CdO powder were dissolved and the solution became clear, 1.5 g Trioctylphosphine (TOP) was injected. When the temperature reached 350 °C, selenium (Se) precursor (0.058g Se+0.36g TOP) was swiftly injected and after 5 s, the reaction was stopped by removing the heating mantle. The CdSe seed was precipitated by ethanol and re-dissolved in chloroform for further use. The resulting CdSe QDs have a lowest exciton peak at 520 nm

(corresponding to 2.6 nm core diameter[2]) and the concentration of CdSe was determined from published extinction coefficient.[3]

CdSe/CdS dot-in-rod and CdS NRs: The CdSe/CdS dot-in-rod (DIR) and CdS NRs were synthesized following a seeded growth method.[1,4] The synthesis of CdSe seed was described above. The OA capped wurtzite CdS seed were synthesized following a literature procedure[5]. To grow the CdS shell, 0.29 g ODPA, 0.08 g hexylphosphonic acid (HPA), 0.06 g CdO and 3 g TOPO were mixed in a 25mL flask and heated to 300°C under Argon flow. After CdO powder were fully dissolved and the solution became clear, 1.5 g Trioctylphosphine (TOP) was injected and the temperature was raised to 350 °C. CdSe (or CdS) seeds (0.8 µmol) and S precursor (0.12 g S in 1.5 g TOP) were swiftly injected. After 8 minutes, the heating mantle was removed and CdSe/CdS (or CdS) NRs were precipitated with ethanol and redispersed in chloroform for future use. The resulting CdSe/CdS NRs have a lowest exciton peak at 565 nm and an emission spectrum centered at 575 nm. The TEM images (Fig. 1) indicates that these NRs are 37.3 ± 2.3 nm in length and 3.0 ± 0.2 nm in diameter as shown in Fig. S1A. From the TEM image of CdS NRs (Fig. 1), we obtained an average length of 31.9 ± 2.4 nm and average diameter of 2.8 ± 0.2 nm (Fig. S1B).
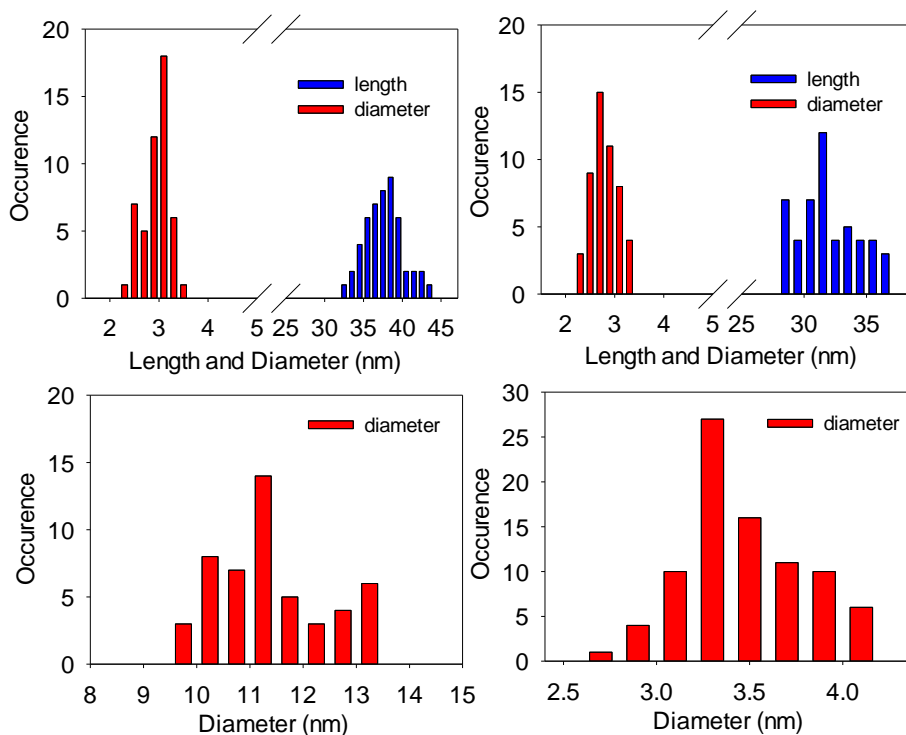

Fig. S1. The size (length and diameter for NRs and diameter for QDs) distribution for (A) CdSe/CdS DIR, (B) CdS NR, (C) CdSe/CdS CS-SV (D) CdSe/CdS CS-SE.

CdSe/CdS core/shell QDs: The CdSe/CdS core/shell QDs were grown by successive ion layer adsorption and reaction (SILAR) method.[6] A cadmium precursor solution (0.1 M) was

prepared by dissolving 0.064 g of CdO in 2.5 mL of oleic acid (OA) and 7 mL of 1-octadecene (ODE) at 300 °C to obtain a colorless solution. The precursor solution was then maintained at above 100 °C. A sulfur injection solution (0.1 M) was prepared by dissolving 32 mg of sulfur in 10 mL of ODE in an ultrasonic bath. The CdS shells were grown one layer at a time, by the successive injection of calculated amounts of cadmium and sulfur solutions using air-free syringe pump (with a rate of 1mL/h). The CdSe/CdS core/shell QDs of similar energy (CS-SE) was prepared by monitor emission peak evolution until it agrees with that of CdSe/CdS DIR, as shown in SI2. The TEM images of CdSe/CdS CS-SE QDs are shown in Fig. 1, from which we obtained a diameter of 3.4 ± 0.3 nm (Fig. S1D). To grow giant CdSe/CdS core/shell QDs of similar volume (CS-SV) as DIR, the amount of Cd and S precursors required was estimated from the desired CdS shell volume. The shell growth was performed initially at 180 °C to maintain the core size and gradually increased up to 240 °C. The time interval between two successive injections was 20 minutes. After purification and precipitation, CdSe/CdS QDs were re-dissolved in chloroform for further measurements. The TEM image of the gaint CdSe/CdS QDs are shown Fig. 1, from which we obtained a diameter of 11.4 ± 0.4 nm (Fig. S1C). The average volume of these QDs is ~2 times bigger than CdSe/CdS DIR.

Ligand exchange to make water soluble NCs: The NCs prepared above were transformed into water by ligand exchange with 3-mercaptopropionic acid (MPA).[7] Excess amount of MPA (20μL) was dissolved in 10 mL methanol and the pH of the solution was adjusted to above 10 with tetramethylammonium hydroxide. A few mg NCs were added and the solution was refluxed at 70°C overnight with N_2 in dark. The MPA capped NCs were precipitated with ethyl acetate and isolated by centrifugation and decantation. After drying, the precipitate was redissolved in water for further use.

PVA-Pt synthesis: Pt particles used as the catalyst for hydrogen evolution were synthesized by thermal reduction of H_2PtCl_6 with citrate[8]. After refluxing the solution for 4h, excess citrate was removed by Amberlite-MB-1 exchange in an ice bath. After filtration, Polyvinyl alcohol (PVA, mass ratio PVA/Pt = 1/1) was added as protective agent and the solution was stirred overnight. The concentration of Pt in reaction solution for H_2 evolution was estimated to be ~ 0.8 mM based on reported extinction coefficient.[9]

Instruments for characterization

UV-Vis spectra were acquired using Agilent 8453 spectrometer equipped with a diode-array detector. The emission spectrum was recorded using FluoroMax 3 spectrofluorimeter. The transmission electron microscopy (TEM) images were acquired with JEOL JEM-1400 (120 kV). The femtosecond and nanosecond transient absorption (TA) and time-resolved fluorescence spectrometers used for these studies have been described elsewhere.[10,11] To correct for slight difference of excitation intensity of the data acquired by fs and ns instruments under the single exciton conditions, the signal size of the ns kinetics was slightly scaled such that these transient kinetics overlap at 0.6-1.4 ns. For all TA measurements, the samples were kept in a 1 mm cuvette and constantly stirred by a magnetic stirrer to avoid photodegradation. Time-resolved fluorescence decay was measured by time-correlated-single photon counting. The excitation wavelength is fixed at 400 nm for all TA measurements and the number of photons per NC is much less than 1 so that the contribution of multiexciton states is negligible.

Sample preparation. The samples for NC-MV^{2+} charge recombination study were prepared by adding a drop of concentrated MV^{2+} methanol solution into a NC chloroform solution followed by sonication. After filtration to remove excess amount of unabsorbed MV^{2+}, the transparent samples were used for TA measurement. The aqueous samples for NC-MV^{2+} with MPA used for charge separation and transient quantum yield measurement were prepared in the same way as those for steady state MV^{2+} photoreduction experiment except for the four times lower NC concentrations.

MV^{2+} photoreduction measurement

Light-driven MV^{2+} reduction was performed in a standard threaded-top fluorescence cuvette (Spectrocell, RF-3010-T) with a total volume of ~3 ml and a path-length of 1 cm. The cuvette was filled with 2.0 ml reaction solutions of sensitizers (concentration to be specified below), MV^{2+} (5.0 mM), sacrificial electron donor (50 mM) (MPA for NCs and Triethanolamine (TEOA) for Ru(bipy)$_3^{2+}$; both neutralized to 7 with HCl or NaOH before mixing) and buffer (50 mM phosphate, pH 7.8). In order to ensure same photon absorption rate, the concentrations of sensitizers were adjusted to have the same absorbance at the illumination wavelength (Abs = 1.1 at 455nm) for all samples. Based on the estimated extinction coefficients (Fig. 1), the actual sensitizer concentrations were ~10.0, 0.43, 3.0, 0.20, 0.2 and 100 μM for CdSe seed, CdS NR, CdSe/CdS CS-SE, CdSe/CdS CS-SV, CdSe/CdS DIR, and Ru(bipy)$_3^{2+}$, respectively. The reaction cells were sealed with a rubber septum, degassed and filled with Argon. The removal of oxygen was confirmed with HP5890A model gas chromatograph equipped with a thermal conductivity detector and a HP-MOLESIEVE capillary GC column (30m × 0.535 mm × 25.00 μm) packed with 5Å molecular sieves. The integrity of the seal was tested by monitoring the absorption spectra reduced MV$^{+·}$ in dark, which shows slightly (~5%) decrease after 1 h. All procedures were performed with a minimum exposure to ambient light. Before illumination, the UV-Vis absorption spectrum of the solution was taken as zero time. The reaction was initiated by unblocking the stabilized LED-light source (λ = 455 nm; light intensity 2.4 mW, beam diameter ~0.4 cm) with constant stirring of the solution (by a magnetic stirrer). The UV-Vis absorption spectra of the solution were taken after desired duration of illumination (seconds), interrupting the illumination by less than 20 s for each spectrum recording. Error bars on MV$^{+·}$ concentrations were calculated from at least two independent experiments.

The MV$^{+·}$ generation quantum yield for these sensitizers is defined as $\Phi_{MV} = \Delta(MV^{+·})/\Delta(\hbar v)$ where $\Delta(MV^{+·})$ is the MV$^{+·}$ generation rates and $\Delta(\hbar v)$ is the photon absorption rates by the reaction solution, respectively. MV$^{+·}$ generation rates $\Delta(MV^{+·})$ were obtained from the slope of the initial three points including 0, 2 and 5s. The photon absorption rate $\Delta(\hbar v)$ was calculated from the illumination power and the absorbance of the reaction solution. The illumination power (2.4 mW) was measured at the front of the reaction cell using a digital laser power meter (OPHIR, model NOVA II). The amount of absorbed light are determined from sample absorbance (OD = 1.10 at 455 nm), the measured power and the estimated refletion/scattering loss of the cuvette front window. The loss of an empty cell was determined to be 14% by UV/Vis spectrometer, from which we assume a 7% loss for each window. The absorbed light intensity is $2.4*0.93*(1-10^{-1.1})$ mW.

H$_2$ generation measurement

The H$_2$ generation reaction was performed in a cylindrical cuvette (NSG, 32UV10) with a total volume of ~2.5 ml following the same operation procedures as the MV^{2+} reduction experiment described above. The reaction volume (2.0 ml) and the concentrations of MV^{2+}, NCs and MPA remain unchanged. A different buffer (50 mM phosphate, pH 6.2) and a higher light intensity (8.0 mW) were used and Pt nanopartilces (0.8 mM) were added as the H$_2$ evolution catalysts

Analysis of H$_2$ in the reaction headspace was performed using a HP5890A model gas chromatograph equipped with a thermal conductivity detector and a HP-MOLESIEVE capillary GC column (30m x 0.535 mm x 25.00 µm) packed with 5Å molecular sieves. Argon was used as a carrier gas. Typically, the H$_2$ amount was quantified by withdrawing a gas sample from the headspace without stopping the reaction. Error bars on H$_2$ were calculated from at least two independent experiments.

Quantum yield for H$_2$ generation is defined as $\Phi_{MV} = 2\Delta(H_2)/ \Delta(\hbar v)$ where $\Delta(H_2)$ is the H$_2$ generation rates. For external quantum yield, $\Delta(\hbar v)$ is calculated from the power of the incident light (8.0 mW). To estimate the internal quantum yield, the photon loss has to be corrected. The loss comes from three processes: 1) scattering and reflection of cuvette front window (~9% loss), 2) scattering of suspended NCs in water, and 3) absorption by the Pt catalyst. The absorbance of Pt and NCs at 455 nm are 0.8 and 1.1, respectively, from which the light intensity absorbed by sensitizer was estimated to be 8.0*0.91*1.1/(1.1+0.8) mW. Because the scattering loss of the suspension is not taken into account, the estimated internal quantum yield should be taken as the lower limit.

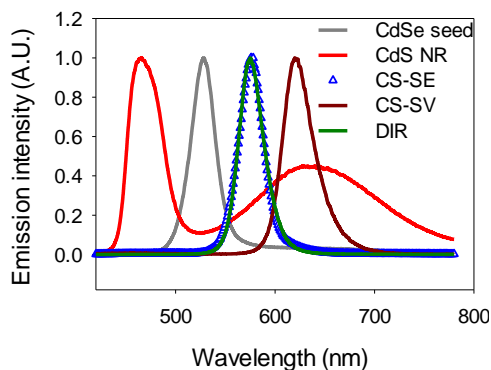## SI 2. Emission spectra of nanocrystals

Fig. S2. Emission spectra of the CdSe seed, CdS NR, CdSe/CdS CS-SE, CdSe/CdS CS-SV and CdSe/CdS DIR used in this study.

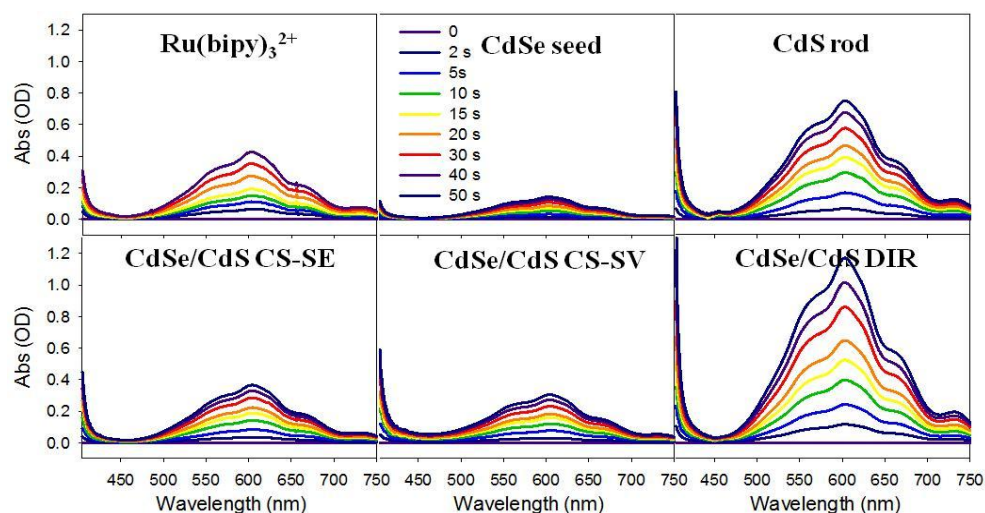## SI 3. Steady-state difference UV-Vis spectra of MV^{2+} photo-reduction

Fig. S3. Steady state UV-Vis difference spectra （0-50 s） showing MV^{2+} photoreduction processes using different sensitizers. Experiment conditions are listed Fig. 2A caption in the main text.

SI 4. MV^+ radical generation kinetics under different MV^{2+} concentrations for $Ru(bipy)_3^{2+}$ and CdSe/CdS DIR.
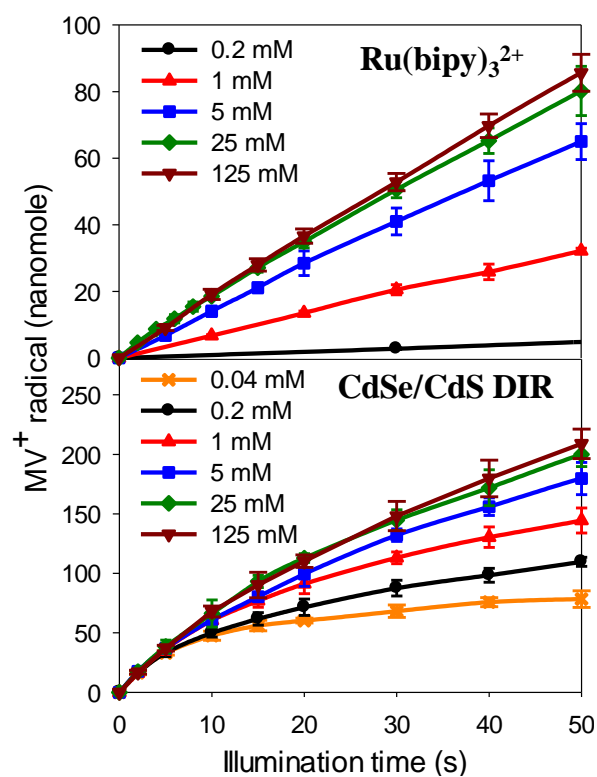
Fig. S4. MV^+ radical generation kinetics in the first 50 s using indicated MV^{2+} concentrations for $Ru(bipy)_3^{2+}$ (upper panel) and CdSe/CdS DIR (lower panel). The amount of $MV^{+\bullet}$ radicals generated for $Ru(bipy)_3^{2+}$ using 0.04 µM MV^{2+} is below the detection limit.

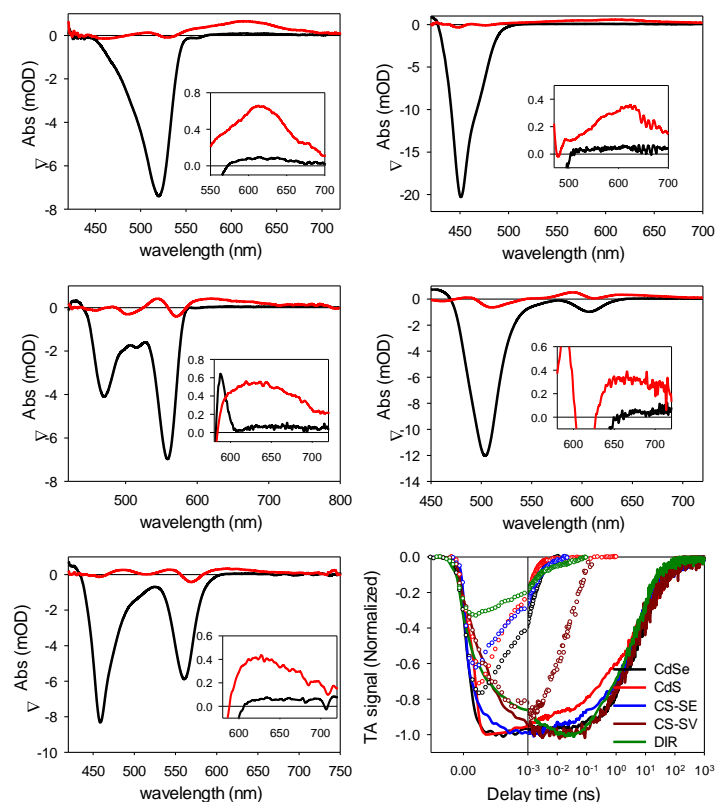## SI 5. TA spectra of MPA-NC with and without MV^{2+} in aqueous solution.

Fig. S5. (A-E)TA spectra of free NCs (black line) and NC-MV^{2+} complexes (red line) for ((A) CdSe seed (10-15 ps), (B) CdS NR (20-30 ps), (C) CdSe/CdS CS-SE (20-30 ps), (D) CdSe/CdS CS-SV (500 ps) and (E) CdSe/CdS DIR (10-20 ps) at indicated delay times (in parentheses) after 400 nm excitation. The MV^+ radical absorption reaches maximum at these delay times in the MPA-NC-MV^{2+} complexes. Insets: expanded views of the TA spectra showing the photo-generated $MV^{+\bullet}$ radical absorption band at >600 nm. (F) Transient bleach recovery kinetics of the lowest energy exciton bands in MPA-NCs with (circles) and without (lines) MV^{2+}, showing long-lived conduction band electrons in free NCs and ultrafast electron transfer in NC-MV^{2+} complexes. For comparison, the transient kinetics of each NC with and without MV^{2+} were taken under the same excitation intensity. The transient kinetics of free NCs (without MV^{2+}) were normalized to 1 at the maximum signal size and the kinetics for the corresponding NC/MV^{2+} complexes were normalized by the same scaling factors. The x-axis is in linear scale from -0.5 to 1 ps and in logarithmic scale from 1 ps to 1 µs.

SI 6. Charge recombination kinetics of NC-MV^{2+} complexes in chloroform.
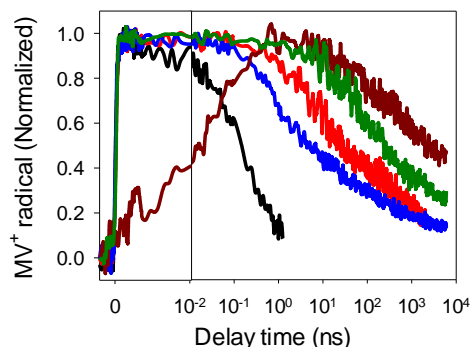

Fig. S6. Normalized MV$^{+\bullet}$ radical formation and decay kinetics of NC-MV^{2+} complexes in chloroform: CdSe seed (black), CdSe/CdS CS-SE (blue), CdS NR (red), CdSe/CdS DIR (dark green) and CdSe/CdSe CS-SV(dark red). The x-axis is in linear scale from -2 − 10 ps and in logarithmic scale from 10 ps to 10 μs.

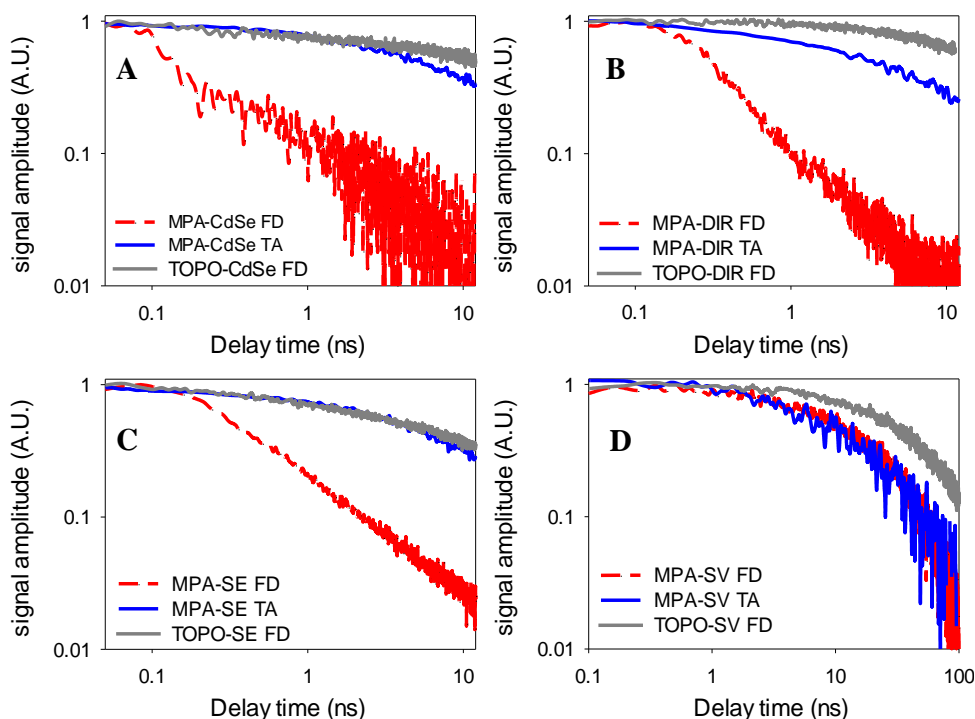**SI 7. Hole filling time by MPA**

Fig. S7. Comparison of fluorescence decay (red) and transient bleach recovery (blue) of the lowest energy exciton absorption band in MPA-capped NCs and fluorescence decay of TOPO-capped NCs (grey) for CdSe seed (A), CdSe/CdS DIR (B), CdSe/CdS CS-SE (C), and CdSe/CdS CS-SV (D).
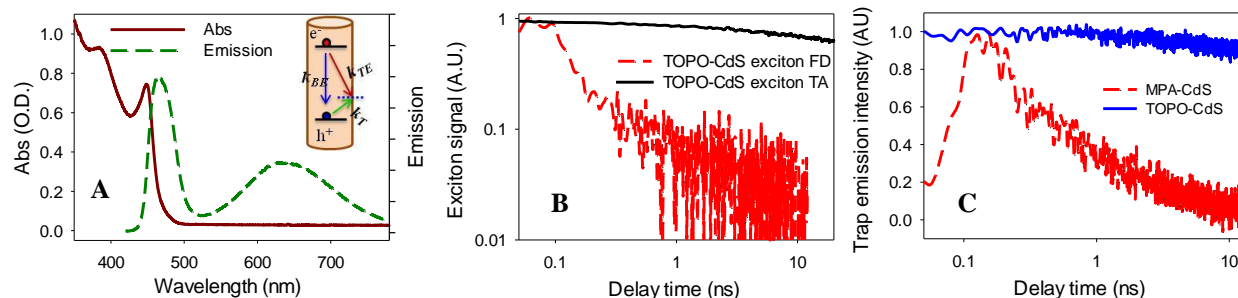
SI 8. Hole trapping and transfer in CdS nanorod

Fig. S8. (A) UV-Vis absorption and emission spectra of CdS NRs. The mission spectrum shows both a band edge and trap state emission. Inset: the competition of band edge (k_{BE}) and trap state (k_{TE}) emission due to the hole trapping process (k_T) (B) Comparison of transient bleach recovery kinetics (black line) and fluorescence decay (red dashed line) of the 1Σ exciton band of CdS NRs. The long-lived conduction band electron and ultrafast exciton emission decay indicates ultrafast trapping of the valence band hole. (C) Comparison of CdSe NR trap emission decay in the absence (blue, in CHCl$_3$) and presence of MPA (red, in water), showing a much faster decay in the latter due to the filling of trapped holes by MPA.

Unlike other NCs described above, CdS NRs show two distinct emission bands with comparable intensity. The band centered at 466 nm can be assigned to CdS band edge emission and the broad band from 500 to 800 nm can be assigned to trap state emission, as shown in Fig. S2. The band edge emission shows an instrument response limited (<100 ps) decay (red line in Fig. S8 B) while the transient absorption bleach recovery of the lowest energy exciton has a half-life time of ~ 100 ns, indicating a long lifetime for the conduction band electrons.[12] Thus, the ultrafast fluorescence decay indicates an ultrafast trapping of the valance band hole. To measure the filling of the trapped hole by MPA, we compare the trap emission in CdS NRs in the presence and absence of MPA, as shown in Figure S8C. The fast trap emission decay in the presence of MPA indicates the transfer of the trapped hole to MPA.

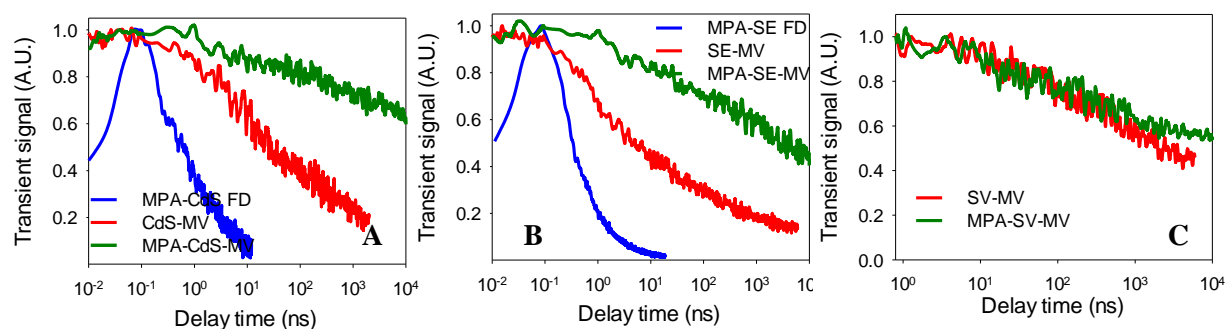## SI 9. Comparison of charge recombination and hole filling in NCs.

Fig. S9. Comparison of fluorescence decay kinetics of MPA-NC (blue line, due to hole transfer to MPA) and $MV^{+\bullet}$ decay kinetics (due to charge recombination) in $NC-MV^{2+}$ complexes in chloroform (red line) and in $MPA-NC-MV^{2+}$ complexes(green line) for CdS NR (**A**), CdSe/CdS CS-SE (**B**) and CdSe/CdS CS-SV (**C**). The slower $MV^{+\bullet}$ decay in $MPA-NC-MV^{2+}$ complexes can be attributed to the removal of holes by MPA. Hole filling kinetics in CdSe/CdS CS –SV is too slowed to be measured by fluorescence decay and is not shown.

References

(1)   Carbone, L.; Nobile, C.; De Giorgi, M.; Sala, F. D.; Morello, G.; Pompa, P.; Hytch, M.; Snoeck, E.; Fiore, A.; Franchini, I. R.; Nadasan, M.; Silvestre, A. F.; Chiodo, L.; Kudera, S.; Cingolani, R.; Krahne, R.; Manna, L. *Nano Lett.* **2007**, *7*, 2942.

(2)   Yu, W. W.; Qu, L. H.; Guo, W. Z.; Peng, X. G. *Chem. Mater.* **2003**, *15*, 2854.

(3)   Jasieniak, J.; Smith, L.; Embden, J. v.; Mulvaney, P.; Califano, M. *J. Phys. Chem. C* **2009**, *113*, 19468.

(4)   Talapin, D. V.; Nelson, J. H.; Shevchenko, E. V.; Aloni, S.; Sadtler, B.; Alivisatos, A. P. *Nano Lett.* **2007**, *7*, 2951.

(5)   Yu, W. W.; Peng, X. G. *Angew. Chem. Int. Ed.* **2002**, *41*, 2368.

(6)   Li, J. J.; Wang, Y. A.; Guo, W.; Keay, J. C.; Mishima, T. D.; Johnson, M. B.; Peng, X. *J. Am. Chem. Soc.* **2003**, *125*, 12567.

(7)   Aldana, J.; Wang, Y. A.; Peng, X. G. *J. Am. Chem. Soc.* **2001**, *123*, 8844.

(8)   Brugger, P. A.; Cuendet, P.; Graetzel, M. *J. Am. Chem. Soc.* **1981**, *103*, 2923.

(9)   Henglein, A.; Ershov, B. G.; Malow, M. *J. Phys. Chem.* **1995**, *99*, 14129.

(10)   Zhu, H.; Song, N.; Lian, T. *J. Am. Chem. Soc.* **2011**, *133*, 8762.

(11)   Song, N.; Zhu, H.; Jin, S.; Zhan, W.; Lian, T. *ACS Nano* **2011**, *5*, 613.

(12)   Klimov, V. I. *Annu. Rev. Phys. Chem.* **2007**, *58*, 635.